Numerical relativity

Bernardo Veronese

November 12, 2024

Why numerical relativity

- Symmetries $\rightarrow$ analytical solutions
  - Black holes (Schwarzschild, Kerr, ...), FLRW cosmologies...
- Perturbation theory
  - Cosmology
  - Black holes
- Small-parameter expansions
  - Post-newtonian theory, v/c
  - Self-force expansion, q
- How do we study high-velocity sources that generate strong fields?
  - Solving Einstein's equations on the computer!

Breakthroughs: some memorable dates

- 1952: french mathematician Yvonne Choquet-Bruhat proved that the Cauchy problem for general relativity is well-posed [Fourès-Bruhat, 1952]: local existence and uniqueness of solutions.
- 1962: Arnowitt, Deser and Misner reformulated the Einstein equations in a Hamiltonian description and explicit 3+1 decomposition. A republished version of their paper is available online [Arnowitt et al., 2008].
- 1964: First numerical experiment in 2D by Hanhn & Lindquist on the IBM 7090 supercomputer [Hahn and Lindquist, 1964].
- 1993: Critical phenomena in gravitational collapse of a scalar field [Choptuik, 1993]
- 1993: Simulation of two black holes colliding [Anninos et al., 1993]
- 1999: First binary neutron star merger in GR [Shibata and Uryū, 2000]

Breakthroughs: first simulation of binary black hole merger

First simulation of a binary black hole system through inspiral, merger and ringdown by [Pretorius, 2005]. Using co-rotating coordinates, the black holes are kept fixed on the grid.

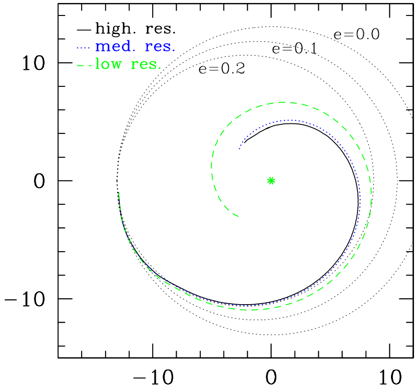

Figure: Slice on the $x - y$ plane of the final orbit of one black hole relative to another (center) for different resolutions in Pretorius' simulations. Extracted from [Pretorius, 2005].

Breakthroughs: gravitational waves from simulations

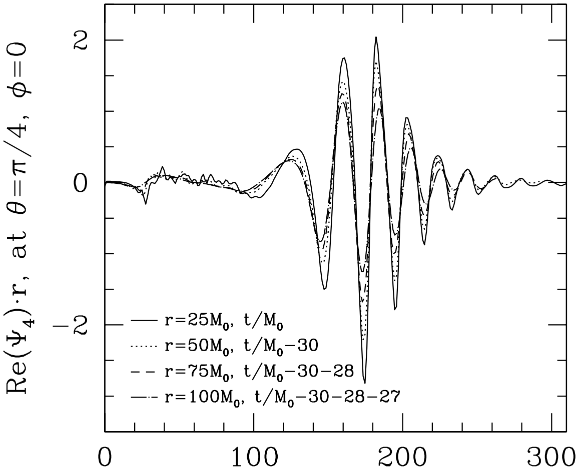

Figure: The waveform extracted at fixed θ and different radii r in Pretorius' simulations. Extracted from [Pretorius, 2005].

Breakthroughs: moving puncture

Coordinate choice where singularities move between gridpoints allows simulations to run for longer [Baker et al., 2006a, Campanelli et al., 2006].

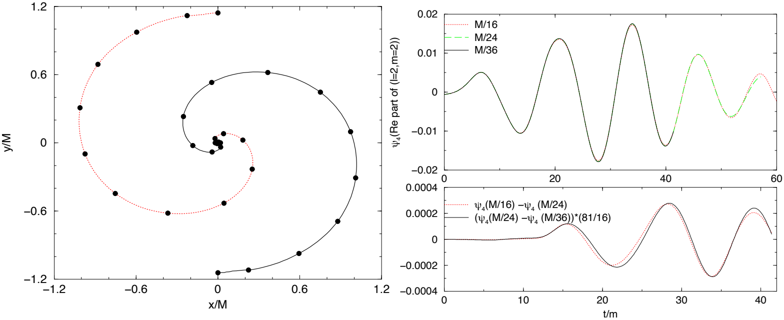

Figure: Extracted from [Campanelli et al., 2006].

Breakthroughs: moving puncture

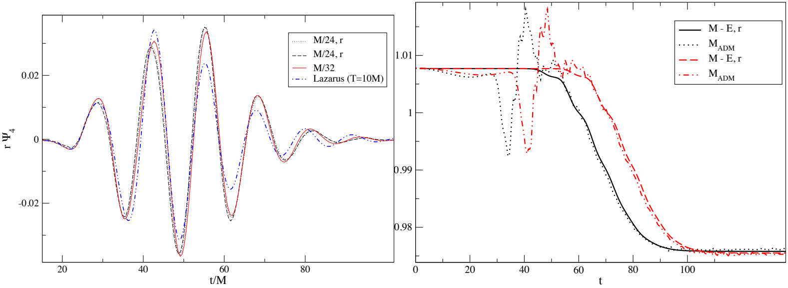

Figure: Extracted from [Baker et al., 2006a]. The figure on the right demonstrates energy conservation throughout the simulation.

The 3+1 decomposition I

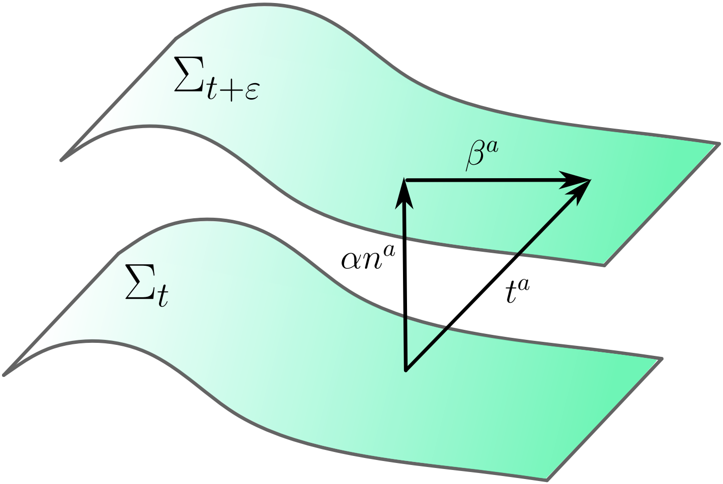

Figure: Extracted from [Hilditch, 2024].

The 3+1 decomposition II

Coordinates $x^\mu = (t, x^i)$. We consider a *foliation* of spacetime, dividing into spacelike hypersurfaces Σ_t, labelled by the coordinate t.

The future-directed unit normal to slices of of constant t can be defined as

$$n^a = -\alpha \nabla^a t, \tag{1}$$

where $\alpha^{-2} = \nabla^a t \nabla_a t$ is the *lapse function*, ensuring $n_a n^a = -1$.

We may define a projector orthogonal to n^a as

$$\perp^a_b = \delta^a_b + n^a n_b. \tag{2}$$

The projector induces a metric $\perp^c_a \perp^d_b g_{ab}$ on Σ_t,

$$\gamma_{ab} = g_{ab} + n_a n_b. \tag{3}$$

The 3+1 decomposition III

We decompose the partial derivative $t^a \equiv (\partial_t)^a$ onto the normal vector and a vector living in the spatial slice,

$$(\partial_t)^a = \alpha n^a + \beta^a. \tag{4}$$

The spatial vector β^i is called the *shift vector*. The line element becomes

$$ds^2 = -\alpha^2 dt^2 + \gamma_{ij}(dx^i + \beta^i dt)(dx^j + \beta^j dt). \tag{5}$$

α, β^i encode the gauge freedom in the theory.
One may define a covariant derivative associated to the metric, $D_a \gamma_{bc} = 0$. From that, the Levi-Civita connection Γ^a_{bc}, the Riemann tensor R^a_{bcd}, the Ricci tensor R_{ab}, and Ricci scalar R.
Note: The full spacetime counterparts have a (4) superscript, ${}^{(4)}R^a_{bcd}, {}^{(4)}R_{ab}, {}^{(4)}R$, etc.

The 3+1 decomposition IV

R^a_{bcd} encodes information about the curvature intrinsic to the slice Σ_t. How it is shaped in the embedding space is encoded in the extrinsic curvature tensor,

$$K_{ab} = -\frac{1}{2}\mathcal{L}_{\mathbf{n}}\gamma_{ab}. \tag{6}$$

One can show that this definition is equivalent to

$$K_{ab} = -\gamma^c_a \gamma^d_b \nabla_{(c} n_{d)}. \tag{7}$$

The 3+1 decomposition V

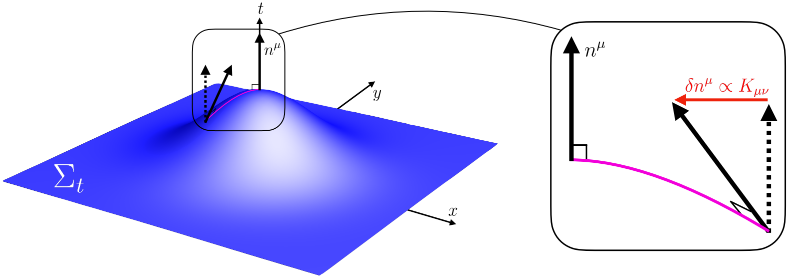

Figure: Extracted from [Aurrekoetxea et al., 2024].

Geometric relations

Taking projections of ${}^{(4)}R_{abcd}$ onto the slice Σ_t, we deduce the Gauss equation

$$R_{abcd} + K_{ac}K_{bd} - K_{ad}K_{bc} = \gamma_a^p \gamma_b^q \gamma_c^r \gamma_d^s \, {}^{(4)}R_{pqrs}. \tag{8}$$

Taking projections of the Riemann tensor onto the slice Σ_t and once onto its normal direction, we deduce the Codazzi equation

$$D_b K_{ac} - D_a K_{bc} = \gamma_a^p \gamma_b^q \gamma_c^r n^s \, {}^{(4)}R_{pqrs}. \tag{9}$$

The last remaining projection yields Ricci's equation,

$$\mathcal{L}_{\mathbf{n}} K_{ab} = n^d n^c \gamma_a^q \gamma_b^r \, {}^{(4)}R_{drcq} - \frac{1}{\alpha} D_a D_b \alpha - K_b^c K_{ab}. \tag{10}$$

The ADM equations

We define $\rho = n_a n_b T^{ab}$, $S^i = -\gamma^{ij} n^a T_{aj}$, $S_{ij} = \gamma_{ia}\gamma_{jb} T^{ab}$, $S = \gamma^{ij} S_{ij}$. Using the Gauss-Codazzi-Ricci relations, we recast the Einstein equations into

$$
\begin{aligned}
0 = \mathcal{C}_0 &\equiv R + K^2 - K_{ij}K^{ij} - 16\pi\rho && (11)\\
0 = \mathcal{C}^i &\equiv D_j(K^{ij} - \gamma^{ij}K) - 8\pi S^i && (12)\\
\partial_t \gamma_{ij} &= -2\alpha K_{ij} + \mathcal{L}_{\boldsymbol{\beta}}\gamma_{ij} && (13)\\
\partial_t K_{ij} &= \alpha(R_{ij} - 2K_{ik}K^k_j + KK_{ij}) - D_i D_j \alpha && (14)\\
&\quad - 8\pi\alpha\left[S_{ij} - \frac{1}{2}\gamma_{ij}(S - \rho)\right] + \mathcal{L}_{\boldsymbol{\beta}} K_{ij}
\end{aligned}
$$

$\mathcal{C}_0$ is the Hamiltonian constraint, $\mathcal{C}_i$ is the momentum constraint. The other two equations evolve γ_{ij} and K_{ij}.

Free-evolution

- One can show that, if the Hamiltonian and momentum constraints are satistfied on an initial hypersurface Σ_0, they will also be satisfied along the evolution (dynamics are constraint-preserving).
- In practice, what is often done is to solve the constraints on Σ_0, and then evolve the other two equations freely.
- Continuum limit: exact. Finite-differencing + floating-point error: constraint violations.

The initial-value problem

- In many relevant systems studied in numerical relativity, spacetime is assymptotically flat $\rightarrow$ natural to formulate bondary conditions at spatial infinity (i.e vanishing fields).
- Example of well-posed bondary value problem: the Laplace equation (elliptical).
- Change of variables to get a better behaved PDE!

Most strategies to obtain a good PDE system involve the conformal decomposition

$$\gamma_{ij} = \psi^4 \tilde{\gamma}_{ij}. \tag{15}$$

Roughly speaking, one specifies the matter content, $\tilde{\gamma}_{ij}$ and K, while solving for ψ and the trace-free part of K_{ij}.

Brill-Lindquist initial data

Let us restrict to vacuum and choose $\tilde{\gamma}_{ij} = \delta_{ij}$. Restrict to time-symmetric initial data $\Rightarrow K_{ij} = 0$ since $K_{ij} \propto \mathcal{L}_{\mathbf{n}}\gamma_{ij}$. Then

1. The momentum constraint is trivially $\mathcal{C}_i = 0$;
2. The hamiltonian constraint is $\nabla^2\psi = 0$.

Laplace equation! By assymptotic flatness, $\psi(r \to \infty) \to 1$. A simple solution on $\mathbb{R}^3 \backslash \mathcal{B}$ (minus a ball) is

$$\psi = 1 + \frac{M}{2r}. \tag{16}$$

The metric γ_{ij} is the spatial part of Schwarzschild in isotropic coordinates! Plus, by linearity,

$$\psi_{\mathrm{BL}} = 1 + \frac{1}{2}\sum_{i=1}^{N} \frac{M_i}{|\mathbf{x} - \mathbf{x}_i|} \tag{17}$$

is also a solution [Brill and Lindquist, 1963]. "Fixed black holes."

Puncture initial data

Time-symmetric initial data $\Rightarrow$ no momenta or spins. Hence relax $K_{ij} \neq 0$, with $K = 0$. For $\mathbb{R}^3 \backslash O$ (minus a point), there is an explicit solution: [Bowen and York, 1980, Brandt and Brügmann, 1997]

$$\psi^2 K_{ij} = \frac{3}{2r^2}\left[2P_{(i}n_{j)} - (\delta_{ij} - n_i n_j)P^k n_k\right] + \frac{3}{r^2}\left[\epsilon_{kil}S^l n^k n_j + \epsilon_{jkl}S^l n^k n_i\right]. \tag{18}$$

P_i, S_i momenta and spin!
For a more detailed discussion, refer to [Cook, 2000].

A mathematical detour

We have so far seen:

- How to construct initial data
- How to evolve them in the 3+1 formalism

Can we start running simulations then? Not yet. A PDE is *well-posed* if the problem admits a unique solution and depends continuously on the initial data relative to some norm.
In this direction, a PDE that admits *strong* or *symmetric* hyperbolicity can be shown to be well-posed locally.
For definitions, theorems and more details, see [Friedrich and Rendall, 2000, Hilditch, 2013].

The generalized-harmonic gauge

The ADM equations aren't directly used in practice. We outline some of the formulations below:
Generalized harmonic gauge (GHG): harmonic coordinates are defined by $\Box x^\alpha = -g^{\mu\nu}\Gamma^\alpha_{\mu\nu} = 0$. GHG introduces functions H^α such that

$$\Box x^\alpha = H^\alpha, \tag{19}$$

and modifies the Einstein equations to

$$R_{ab} - \nabla_{(a} C_{b)} = 8\pi G \left(T_{ab} - \frac{1}{2} T g_{ab} \right), \tag{20}$$

where $C_a = \Gamma_a + H_a$ is the harmonic constraint. $C_a = 0$ on initial data $\Rightarrow C_a = 0$ for $t > 0$. Symmetric hyperbolic first order reduction $\Rightarrow$ local well-posedness! See [Lindblom et al., 2006] for more details.

The Z_4 decomposition I

Similar to GHG, the Z_4 decomposition modifies the Einstein equations to [Bona et al., 2003]

$$
\begin{aligned}
&R_{ab} + 2\nabla_{(a}Z_{b)} - \kappa_1[2n_{(a}Z_{b)} - (1+\kappa_2)g_{ab}n_c Z^c] + W_{ab}(Z) \\
&\quad = 8\pi G\left(T_{ab} - \frac{1}{2}Tg_{ab}\right).
\end{aligned} \tag{21}
$$

The EOMs for Z_a in the 3+1 decomposition take the form

$$
\partial_t(n_a Z^a) = \alpha\mathcal{C}_0 + \text{ terms in } Z_a, \tag{22}
$$

$$
\partial_t Z_i = \alpha\mathcal{C}_i + \text{ terms in } Z_a. \tag{23}
$$

$\mathcal{C}_0 = \mathcal{C}_i = Z_a = 0$ at $t = 0 \to$ they are zero always (closed system of constraints).

The Z_4 decomposition II

- The terms proportional to κ_1 are constraint-damping: supress small, high frequency constraint violations $\Rightarrow$ good for numerical stability [Gundlach et al., 2005].
- Does not impose GHG gauge
- Evolved variables are conformally decomposed (good for black holes!)
- Comes in different flavors: BSSN, CCZ4, Z4c
    - BSSN (Baumgarte-Shapiro-Shibata-Nakamura) [Shibata and Nakamura, 1995, Baumgarte and Shapiro, 1998]
    - Z4c [Bernuzzi and Hilditch, 2010]

For further study

Some resources on numerical relativity:

- David Hilditch's review paper 2405.06035
- Numerical Relativity: Solving Einstein's Equations on the Computer (Baumgarte & Shapiro, 2010)
- Introduction to 3+1 Numerical Relativity (Alcubierre, 2008)
- 3+1 formalism and Bases of Numerical Relativity (Eric Gourgoulhon, 2007, very geometric approach, gr-qc/0703035)
- Seminar by Sebastiano Bernuzzi on Youtube (extensive list of resources on his website)

Astrophysics from simulations: black hole kicks

Recoil from gravitational waves may imprint large linear momenta to the remnant black hole [Baker et al., 2006b, Campanelli et al., 2007b, Campanelli et al., 2007a, González et al., 2007].

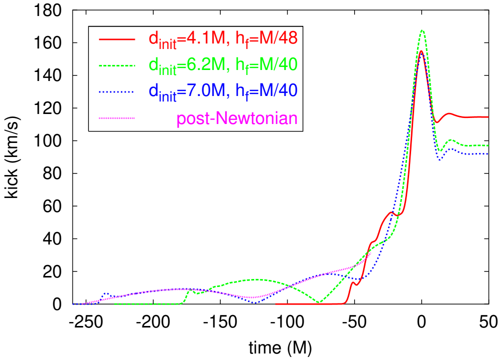

Figure: Recoil velocity for non-spinning black hole binary. Extracted from [Baker et al., 2006b].

Final velocity $v \geq 1000\,\mathrm{km/s}$ if BHs are spinning. Larger than escape velocities of typical clusters? Galaxies? Halos?

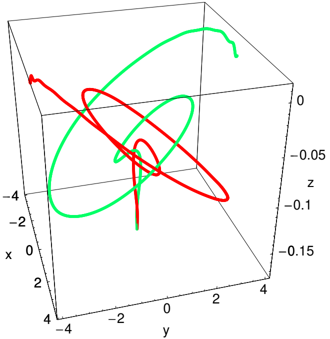

Figure: Extracted from [González et al., 2007].

Calibrating waveforms with numerical relativity

The LIGO-VIRGO-KAGRA collaboration uses different waveform families to fill template banks for searching for gravitational-wave signals. Prominent examples are

- the IMR phenomenological waveforms [Ajith et al., 2011],
- Effective-one-body waveforms [Buonanno and Damour, 1999, Buonanno and Damour, 2000],
- Reduced-order and surrogate models [Tiglio and Villanueva, 2022].

All of these rely on NR waveforms for calibration $\rightarrow$ catalogues of 4000+ simulated GWs exploring the parameter space $(M_1, M_2, \mathbf{S}_1, \mathbf{S}_2)$:

- SXS catalog
- BAM catalog
- RIT catalog
- GeorgiaTech catalog

Extracting gravitational waves from simulations I

A popular method of calculating the waveforms from the simulations use the Newman-Penrose formalism [Newman and Penrose, 1962]. For simplicity, we use a spherical polar basis $\{\mathbf{e}_t, \mathbf{e}_r, \mathbf{e}_\theta, \mathbf{e}_\phi\}$:

$$\mathbf{l} = \frac{1}{\sqrt{2}}(\mathbf{e}_t + \mathbf{e}_s), \mathbf{k} = \frac{1}{\sqrt{2}}(\mathbf{e}_t - \mathbf{e}_s), \mathbf{m}_\pm = \frac{1}{\sqrt{2}}(\mathbf{e}_\theta \pm i\mathbf{e}_\phi). \quad (24)$$

The vectors l^a and k^a are radially outgoing and incoming null. They satisfy $l_a k^a = m_{+,a} m_-^a = 1$, the other inner products vanish. The five Newman-Penrose complex scalars characterize the 10 degrees of freedom contained in the Weyl tensor, the trace-free part of the Riemann tensor. Particularly interesting is the ψ_4 scalar,

$$\psi_4 = -\,{}^{(4)}C_{abcd} k^a m_-^b k^c m_-^d. \quad (25)$$

Extracting gravitational waves from simulations II

Far away from matter sources, we simplify ${}^{(4)}R_{ab} \to 0 \Rightarrow {}^{(4)}C_{abcd} \to {}^{(4)}R_{abcd}$. In the TT gauge, one may show that it takes the simple form

$$\psi_4 = \ddot{h}_+ - i\ddot{h}_\times , \tag{26}$$

completely describing the outgoing gravitational radiation. Some remarks:

- The choice of null tetrad is not unique
- In theory we should compute $\lim_{r\to\infty} r\psi_4$, but simulations cover finite domain $\to$ need interpolation methods at different radii

Gravitational-wave extraction is a subject of its own. For a review, see [Bishop and Rezzolla, 2016].

Simulations of binary neutron star coalescences with radiative and neutrino transfer, electromagnetic emission...

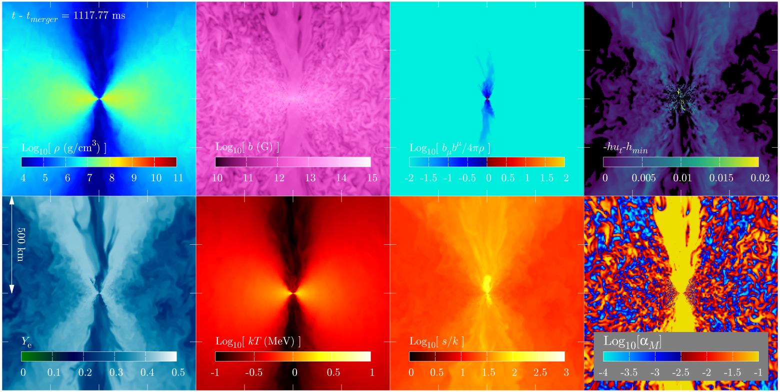

Figure: 1 second before the merger of a GW170817-like binary neutron star. Extracted from [Kiuchi et al., 2023]. See video.

Some topics left out

- Gravitational collapse and critical phenomena
- Simulations in higher dimensions and cosmic censorship
- Applications in cosmology
- Gauge choices
- Finite-differencing methods
- High-performance computing

Numerical relativity in Brazil

- NumRel group (UERJ, 3+ researchers)
- Maximiliano Ujevic (UFABC)

Ajith, P., Hannam, M., Husa, S., Chen, Y., Brügmann, B., Dorband, N., Müller, D., Ohme, F., Pollney, D., Reisswig, C., Santamaría, L., and Seiler, J. (2011).
Inspiral-merger-ringdown waveforms for black-hole binaries with nonprecessing spins.
Phys. Rev. Lett., 106:241101.

Anninos, P., Hobill, D., Seidel, E., Smarr, L., and Suen, W.-M. (1993).
Collision of two black holes.
Phys. Rev. Lett., 71:2851–2854.

Arnowitt, R., Deser, S., and Misner, C. W. (2008).
Republication of: The dynamics of general relativity.
General Relativity and Gravitation, 40(9):1997–2027.

Aurrekoetxea, J. C., Clough, K., and Lim, E. A. (2024).
Cosmology using numerical relativity.

Baker, J. G., Centrella, J., Choi, D.-I., Koppitz, M., and van Meter, J. (2006a).

Gravitational-wave extraction from an inspiraling configuration of merging black holes.
Phys. Rev. Lett., 96:111102.

Baker, J. G., Centrella, J., Choi, D.-I., Koppitz, M., van Meter, J. R., and Miller, M. C. (2006b).
Getting a kick out of numerical relativity.
Astrophys. J. Lett., 653:L93–L96.

Baumgarte, T. W. and Shapiro, S. L. (1998).
Numerical integration of einstein's field equations.
Phys. Rev. D, 59:024007.

Bernuzzi, S. and Hilditch, D. (2010).
Constraint violation in free evolution schemes: Comparing the bssnok formulation with a conformal decomposition of the z4 formulation.
Phys. Rev. D, 81:084003.

Bishop, N. T. and Rezzolla, L. (2016).
Extraction of Gravitational Waves in Numerical Relativity.

Living Rev. Rel., 19:2.

Bona, C., Ledvinka, T., Palenzuela, C., and Žáček, M. (2003).
General-covariant evolution formalism for numerical relativity.
Phys. Rev. D, 67:104005.

Bowen, J. M. and York, J. W. (1980).
Time-asymmetric initial data for black holes and black-hole collisions.
Phys. Rev. D, 21:2047–2056.

Brandt, S. and Brügmann, B. (1997).
A simple construction of initial data for multiple black holes.
Phys. Rev. Lett., 78:3606–3609.

Brill, D. R. and Lindquist, R. W. (1963).
Interaction energy in geometrostatics.
Phys. Rev., 131:471–476.

Buonanno, A. and Damour, T. (1999).
Effective one-body approach to general relativistic two-body dynamics.

Phys. Rev. D, 59:084006.

Buonanno, A. and Damour, T. (2000).
Transition from inspiral to plunge in binary black hole coalescences.
Phys. Rev. D, 62:064015.

Campanelli, M., Lousto, C. O., Marronetti, P., and Zlochower, Y. (2006).
Accurate evolutions of orbiting black-hole binaries without excision.
Phys. Rev. Lett., 96:111101.

Campanelli, M., Lousto, C. O., Zlochower, Y., and Merritt, D. (2007a).
Large merger recoils and spin flips from generic black-hole binaries .
Astrophys. J. Lett., 659:L5–L8.

Campanelli, M., Lousto, C. O., Zlochower, Y., and Merritt, D. (2007b).

Maximum gravitational recoil.
Phys. Rev. Lett., 98:231102.

Choptuik, M. W. (1993).
Universality and scaling in gravitational collapse of a massless scalar field.
Phys. Rev. Lett., 70:9–12.

Cook, G. B. (2000).
Initial data for numerical relativity.
Living Reviews in Relativity, 3(1):5.

Fourès-Bruhat, Y. (1952).
Théorème d'existence pour certains systèmes d'équations aux dérivées partielles non linéaires.
Acta Mathematica, 88(none):141 – 225.

Friedrich, H. and Rendall, A. D. (2000).
The Cauchy problem for the Einstein equations.
Lect. Notes Phys., 540:127–224.

Geroch, R. (1970).

Domain of Dependence.
Journal of Mathematical Physics, 11(2):437–449.

González, J. A., Hannam, M., Sperhake, U., Br¨ ugmann, B., and Husa, S. (2007).
Supermassive recoil velocities for binary black-hole mergers with antialigned spins.
Phys. Rev. Lett., 98:231101.

Gundlach, C., Calabrese, G., Hinder, I., and Martín-García, J. M. (2005).
Constraint damping in the z4 formulation and harmonic gauge.

Classical and Quantum Gravity, 22(17):3767.

Hahn, S. G. and Lindquist, R. W. (1964).
The two-body problem in geometrodynamics.
Annals of Physics, 29(2):304–331.

Hilditch, D. (2013).
An Introduction to Well-posedness and Free-evolution.

Int. J. Mod. Phys. A, 28:1340015.

Hilditch, D. (2024).
Solving the einstein equations numerically.

Kiuchi, K., Fujibayashi, S., Hayashi, K., Kyutoku, K., Sekiguchi, Y., and Shibata, M. (2023).
Self-consistent picture of the mass ejection from a one second long binary neutron star merger leaving a short-lived remnant in a general-relativistic neutrino-radiation magnetohydrodynamic simulation.
Phys. Rev. Lett., 131:011401.

Lindblom, L., Scheel, M. A., Kidder, L. E., Owen, R., and Rinne, O. (2006).
A new generalized harmonic evolution system.
Classical and Quantum Gravity, 23(16):S447–S462.

Newman, E. and Penrose, R. (1962).
An approach to gravitational radiation by a method of spin coefficients.

Journal of Mathematical Physics, 3(3):566–578.

Pretorius, F. (2005).
Evolution of binary black-hole spacetimes.
Phys. Rev. Lett., 95:121101.

Shibata, M. and Nakamura, T. (1995).
Evolution of three-dimensional gravitational waves: Harmonic slicing case.
Phys. Rev. D, 52:5428–5444.

Shibata, M. and Uryū, K. b. o. (2000).
Simulation of merging binary neutron stars in full general relativity: $\Gamma = 2$ case.
Phys. Rev. D, 61:064001.

Tiglio, M. and Villanueva, A. (2022).
Reduced order and surrogate models for gravitational waves.
Living Rev. Rel., 25(1):2.

Can you always foliate a spacetime?

- A spacetime can be foliated if and only if it has a Cauchy surface
- A Cauchy surface is a spacelike hypersurface such that any causal (timelike or null) curve without endpoints intersects it only once
- The domain of dependence of a Cauchy surface is all of spacetime.
- Spacetimes with closed timelike curves evidently do not have a Cauchy surface by the above definition.
- For the curious reader, we refer to [Geroch, 1970].